Regional Studies in Marine Science 31 (2019) 100761

Contents lists available at ScienceDirect

Regional Studies in Marine Science

journal homepage: www.elsevier.com/locate/rsma

Influence of the coastal circulation and water-mass characteristics in structuring the zooplankton community of the eastern Arabian Sea

Kusum Komal Karati [a,*], Ashadevi C.R. [a], Rasheed K. [a], Vineetha G. [b], Smitha B.R. [a], Vimalkumar K.G. [a], Sari Mol C.N. [a], Sudhakar M. [a]

[a] Centre for Marine Living Resources & Ecology, Kochi 682037, India
[b] Central Marine Fisheries Research Institute, Kochi 682018, India

HIGHLIGHTS

- Bay of Bengal water intrusion was observed in the eastern Arabian Sea during winter.
- East India and west India coastal currents influenced the intrusion.
- The intruded water structured the zooplankton community and their abundance.
- Three distinct water masses were observed categorized by discrete salinity and density.
- Copepod species exhibited affinity towards distinct water masses.

GRAPHICAL ABSTRACT

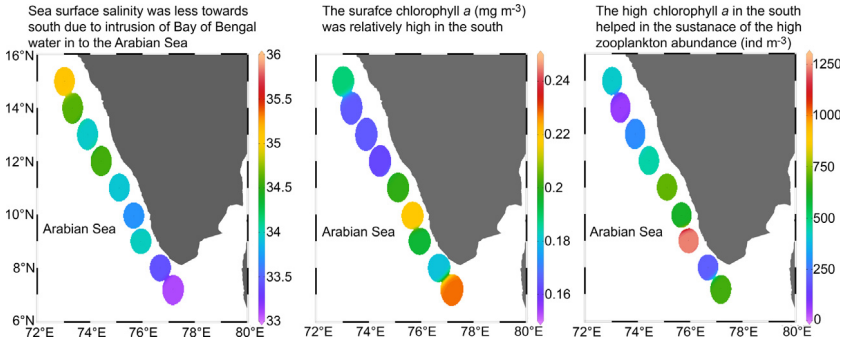

ARTICLE INFO

Article history:
Received 11 January 2019
Received in revised form 30 April 2019
Accepted 12 July 2019
Available online 19 July 2019

Keywords:
Arabian sea
Intrusion
Zooplankton
Copepoda
Water mass
Coastal currents

ABSTRACT

Understanding the forcing mechanisms that determine the coastal ecosystem dynamics has always been a challenging topic of research. The Arabian Sea (AS) coastal ecosystem in the western half of the northern Indian Ocean is influenced by the seasonally reversing atmospheric forcing and structured by distinct water masses along its depth. Although AS differs greatly from its eastern counter-half, Bay of Bengal (BoB) in the thermohaline characteristics, the inter-basin exchanges of the water masses between these ocean basins add complexity to its hydrography. Hence, the present study was attempted to understand the influence of the intrusion of the BoB water in structuring the zooplankton community of the coastal AS. In the mixed layer depth, a conspicuous spatial heterogeneity was noticed in the distribution and abundance of the zooplankton community contributed by the cumulative influence of the higher phytoplankton biomass and the advection of population through BoB water intrusion regulated by the coastal circulation in the southern part. The study also assessed the interaction of the zooplankton community with the specific water masses defined by distinct thermohaline characteristics along the vertical profile of the AS coastal waters. Three distinct water masses were identified within the 200 m depth of AS each categorized by discrete salinity and density features. The distinct groups of the dominant taxon, Copepoda identified through redundancy analysis demonstrate the species-specific preferences of the community to different water mass characteristics in the AS. This study addressing how hydrographic characteristics shape the macroecology of zooplankton in the coastal AS, will add new insight in understanding the dynamic ecosystems of the northern Indian Ocean.

1. Introduction

Marine habitats categorized according to their distance from the shore and depth profiles have a critical role in sustaining

* Corresponding author.
E-mail address: kusum.kk1@gmail.com (K.K. Karati).

https://doi.org/10.1016/j.rsma.2019.100761
2352-4855/

the life on the earth (Barnes and Hughes, 1999). Among the diverse marine habitats, the coastal waters occupying 7% of the oceanic area gains immense significance for their high productivity supporting rich fishing grounds (Pauly et al., 2002). The dynamic coastal currents and their influence in the water mass formation often enunciate variability in the coastal ecology and productivity patterns thereby affecting the economical turnover of the coastal livelihood (Caputi et al., 1996; Eisner et al., 2013). Hence, a comprehensive understanding on the coastal circulation, water mass characteristics and the cumulative influence of these hydrographical attributes on the pelagic community is utmost important while elucidating the productivity and biogeochemical functioning of any coastal ecosystems (Daneri et al., 2000; Luis and Kawamura, 2004).

In the pelagic realm, mesozooplankton forms an important conduit transferring energy from the primary producers to economically exploitable higher trophic levels (Suthers and Rissik, 2009). Zooplankton, because of their sensitivity towards the physicochemical attributes of their habitats often forms an effective tool in tracing the distinct water masses in the marine ecosystem (Bonnet and Frid, 2004; Eisner et al., 2013). Moreover, their feeble locomotive power making their transport and distribution dependent on the ocean currents turns them an ideal indicator of the current movements in the ocean (Hwang and Wong, 2005). Their ecological strategy of high preponderances upon favorable environmental conditions is also a widely observed feature in the global ocean (Thomas and Nielsen, 1994; Karati et al., 2019). Hence it becomes vital to segregate the role of coastal circulation and local population growth in regulating the zooplankton ecology of the dynamic coastal environment. Although the driving forces governing the zooplankton ecology of the Atlantic and Pacific coastal waters are well studied, information pertaining to this aspect is limited from the Indian Ocean (Wiafe and Frid, 1996; Verheye et al., 1998; Ayón et al., 2008).

The Arabian Sea (AS), the western half of the northern Indian Ocean is separated from its eastern counterpart, Bay of Bengal (BoB) by the Indian subcontinent. The productivity pattern of these twin ocean basins is heavily influenced by the seasonally reversing atmospheric forcing which in turn plays a pivotal role in the formation of the distinct water masses and the flow patterns of the coastal currents (Shetye et al., 1991; Gauns et al., 2005). Several water masses contribute to the vertical structure of the AS (Prasanna Kumar and Prasad, 1999; Prasad et al., 2001) and the West India Coastal current (WICC), flowing through the surface along the west coast of India has a critical role in shaping the water mass characteristics of the upper layers of the AS (Shetye et al., 1991). The East India Coastal Current (EICC), a coastal current flowing through the surface waters of the BoB, though geographically positioned in the same latitudinal co-ordinates, differ in the thermohaline characteristics with WICC due to the differences in the locale of origin (Shetye and Shenoi, 1988). During the winter monsoon period, the EICC is considered to feed the WICC subsequently leading to the intrusion of BoB water into the AS (Prasanna Kumar et al., 2004). However, the consequence of this intrusion on the zooplankton community of the coastal AS is mostly unaddressed.

Hence, the study was designed to evaluate the influence of the intrusion of the BoB water in structuring the zooplankton community of the AS. Considering the existence of different water masses in the AS, the association of the zooplankton community with the discrete water masses were also evaluated to understand the spatial heterogeneity in their distribution along both horizontal and vertical scales. The study is the sequel to the studies that dealt with the controlling factors regulating the macroecology of the phytoplankton and zooplankton in the tropical Indian Ocean (Padmakumar et al., 2017; Karati et al., 2018, 2019; Vineetha et al., 2018). As a pioneering study depicting the influence of the intrusion of the BoB water on the mesozooplankton community dynamics of the AS, the results generated will be useful in assessing the ecohydrographic drivers that govern the ecology of mesozooplankton in this important coastal ecosystem in the northern Indian Ocean.

2. Materials and methods

2.1. Sampling

Based on the existing knowledge on the temporal and spatial distribution of salinity in the AS and the expected period of intrusion of BoB water into the coastal AS, the sampling was carried out from 22nd January to 1st February, 2017, the peak winter monsoon period, when the intrusion is expected to be at its maximum. The sampling was carried out onboard FORV Sagar Sampada (Cruise #355 Leg II) as part of the Marine Living Resources (MLR) program in the northern Indian Ocean. A total of 9 stations were fixed at an interval of 1° latitude (7°–15° N) covering the coastal regions of the south-eastern AS (Fig. 1). For maintaining the uniformity in sampling, the depth of sampling of all the stations was maintained at ∼200 m.

A CTD (SBE 911Plus Seabird Electronics, USA) was used to obtain the temperature and salinity profiles of the water column. The CTD was also equipped with a dissolved oxygen (DO) sensor to obtain the DO profiles of the water column. The instrument was operated down to a depth of 200 m at all the sampling stations. Furthermore, to understand the coastal currents along the east and west coast of India and their influence on the intrusion of BoB waters into the AS, the near-real-time surface currents in the region was plotted from https://coastwatch.pfeg.noaa.gov/erddap/.

The MODIS-Aqua satellite ocean color data were used to estimate the surface chlorophyll *a* distribution in the coastal region of the AS (http://giovanni.gsfc.nasa.gov/giovanni). The time-averaged chlorophyll *a* value for the sampling period (22nd Jan 2017 to 1st Feb 2017) was used for the study. For each sampling location, a square (side lengths 1° latitude and 1° longitude) was formed considering the coordinates of the station location as the center of the square. All the data points within the square were computed, and the arithmetical average value was used as the representative chlorophyll *a* for the sampling location.

Zooplankton sampling was carried out using a multiple plankton net (Hydrobios, Germany) with a mouth area of 0.25 m^2 and a mesh size of 200 μm. The net was towed vertically at a speed of 1 m s^{-1} and was operated at prefixed depths by shipboard controls with electronic sensors. Samples were collected from three discrete depths, including the mixed layer depth (MLD), the thermocline (TC), the base of the thermocline (BT) to near bottom (∼200 m). The MLD was determined as the depth up to which a temperature decrease of 0.5 °C occurred from the sea surface temperature. The thermocline base was defined as the depth where the temperature reached 15 °C. The zooplankton samples collected were immediately passed through a 200-μm mesh, and the displacement volume was measured after removing the excess water with an absorbent paper (Harris et al., 2000). The detailed taxonomic analysis and enumeration of the zooplankton taxa were carried out using a stereo zoom microscope (Leica MZ 16). The abundances of the zooplankton taxa were calculated based on the volume of water filtered through the net and was expressed as (ind m^{-3}). Copepoda, being the dominant zooplankton taxon of the coastal AS (Madhupratap and Haridas, 1990; Madhupratap et al., 1996; Padmavati et al., 1998), their detail species-level identification was carried out to get a comprehensive perception of the influence of the BOB intrusion

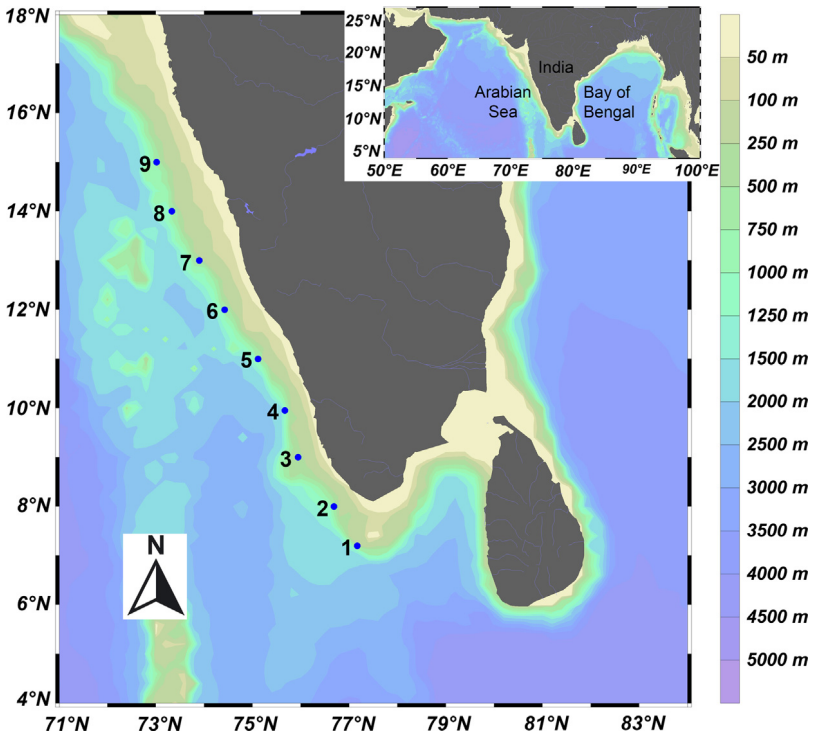

Fig. 1. Distribution of the station locations along the west coast of India in the eastern Arabian Sea.

process in structuring the copepod community of the coastal Arabian Sea. The copepod species-level identification was carried out using a Nikon SMZ645 stereozoom microscope and a Nikon E 400 compound microscope ($\times$40 and $\times$100 magnification) following the standard identification manuals (Kasturirangan, 1963; Sewell, 1999; Conway et al., 2003).

2.2. Statistical analysis

2.2.1. t-test and analysis of variance

To identify the variability in the zooplankton biomass and abundance along different depth strata, one-way ANOVA was performed with two-tailed P-values and 95% confidence intervals. Prior to the analysis, the D'Agostino and Pearson Omnibus normality test was performed to determine whether parametric or non-parametric ANOVA (Friedman test) has to be applied. A t-test was carried out (two-tailed P values and 95% confidence intervals) for the biotic and abiotic variables to assess the significance of variation existing between the northern and southern part of the coastal AS. In case of the t-test also, the parametric and nonparametric analysis (Mann–Whitney test) was selected based on the results of the normality test. Both, the ANOVA and t-test were performed using Graphpad Prism.

2.2.2. Cluster analysis

To assess the similarity in the station locations of the MLD, the agglomerative hierarchical cluster analysis was done based on the abundance of the Copepod species using PRIMER v.7 (Clarke and Gorley, 2015). The analysis was based on the Bray–Curtis similarity matrices of the fourth root transformed abundance of copepod of each sampling location.

2.2.3. β-Diversity

The β-diversity of the Copepoda community was carried out to assess the spatial variation in the community structure (Anderson et al., 2011) and for this, the index of the multivariate dispersion (MVDISP, Warwick and Clarke, 1993) was used. Additionally, the analysis of similarity (one-way ANOSIM) was used to describe the dissimilarities in the Copepoda community among the depth strata.

2.2.4. Biotic–abiotic interrelations

The Bio-Env analysis was carried out using PRIMER 6 to identify the variables that best explain the abundance and distribution of the Copepoda community of the study region. This multivariate analysis is useful in linking the assemblage patterns to the forcing variables (Clarke et al., 2008) and the Spearman rank correlation (ρ) was used for this analysis. As copepod species are predominantly herbivorous or omnivorous (Paffenhöfer and Knowles, 1980), along with temperature, salinity and DO, the chlorophyll *a* was also included as the forcing variable. The redundancy analysis (RDA) was carried out using the copepod species abundance along the depth layers as the response variables and the abiotic variables (temperature, salinity, density and DO) as the explanatory variables.

3. Results

3.1. Coastal currents

The pattern of the geostrophy derived surface currents along the west coast of India was in accordance with the general characteristics of West India Coastal Current (WICC) during the northeast monsoon. During this period, the surface current flowed towards north along the coast (Fig. 2 and Supplementary Fig. 1). In the course of its northward journey, the coastal current exhibited a semicircular deflection towards the offshore along 9° N. A similar small offshore deflection of this northward flow was further noticed along 12° N (Fig. 2). Along the east coast of India, the coastal current flowed towards the south indicating its joining with the northward flow in the west coast (Fig. 2 and Supplementary Fig. 1). From the northern part, the East India coastal current (EICC) in BoB flowed towards south and at the tip of the Srilanka got divided into two arms. One arm flowed

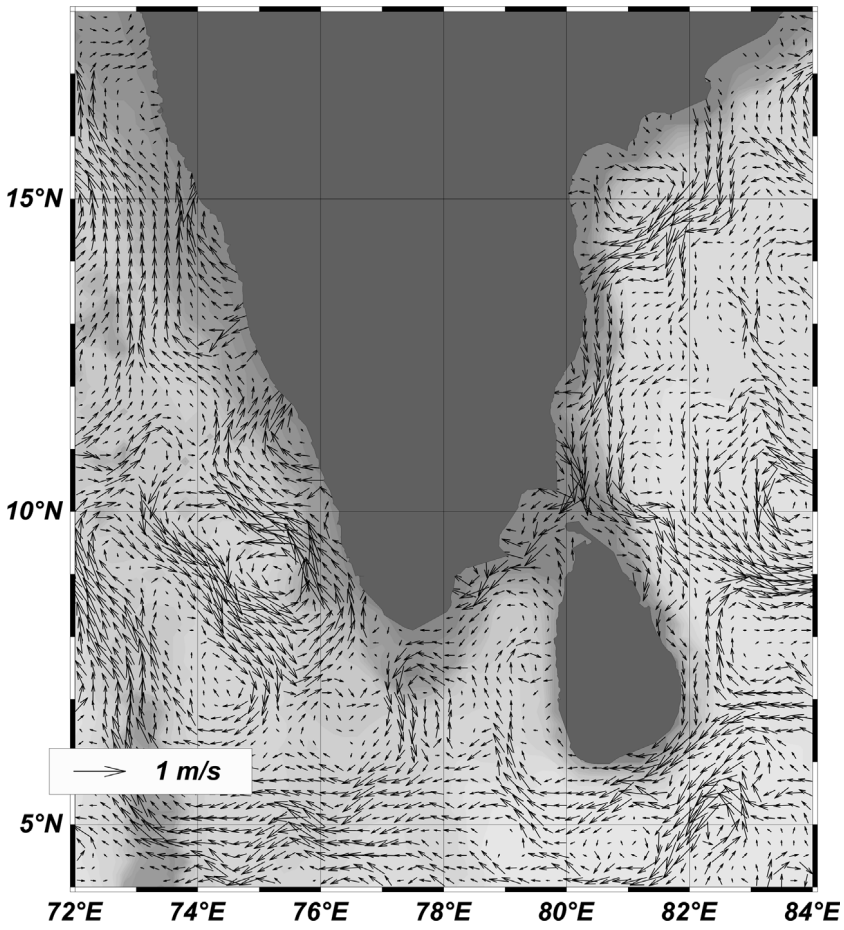

Fig. 2. Distribution of surface currents along the east and west coast of India (Considering the time-lag between physical process and its influence on biotic community, the current structure on 22nd Jan 2017, the initial day of sampling was selected. The detailed current structure for the entire sampling period is available in Supplementary Fig. 1).

through the Palk Strait, the shallow region between India and Srilanka, and joined the northward flowing WICC in the Arabian Sea (Fig. 2). The second arm flowed further south around Srilanka and turned towards north to join with the WICC in the Arabian Sea (Fig. 2).

3.2. Physico-chemical environment

The vertical profile of salinity exhibited a prominent variation both along the depth and latitudes. The low saline water (salinity < 34) characterized by low potential density (<22.5 g cm^{-3}) mostly occurred up to 11° N and up to a thickness of ∼50 m (Fig. 3a, b). The sea surface salinity (SSS, 4 m depth) exhibited a latitudinal gradient with a gradual increase towards the north (Fig. 3a). The SSS in the south (<34, 7° to 11° N, up to which the low-salinity water intrusion was prominent) was lower than that of the north (>34.5) with a significant statistical variation (Mann–Whitney test, $P < 0.05$). Interestingly, a sub-surface high saline water mass (salinity > 35.5) was noticed with relatively more thickness in the north. The potential density and salinity of this water satisfied the characteristic potential density (22.8–24.5 g cm^{-3}) and temperature range (24°–28°C) of the Arabian Sea High Saline Water (Prasanna Kumar and Prasad, 1999), that originates in the northern Arabian Sea (Figs. 3a–c, 4). The deeper water (125–200 m) was relatively less saline (34.5–35.5) compared to the sub-surface water and with a potential density of >24.5 g cm^{-3} formed the Arabian Sea intermediate water (Figs. 3a–b, 4).

The sea surface temperature (SST, 4 m) varied between 27.2° and 28.9 °C. The SST in the south (average ± SD, 28 ±0.6 ° C) was relatively low compared to the north (28.8 ±0.1 °C), and the variation was statistically significant (Mann–Whitney test, $P < 0.05$). Along a vertical scale, the temperature dropped with depth especially below 90 m (Fig. 3c). A temperature inversion was noticed in the vertical profile between depths of 75 m and 100 m at few station locations, most evidently in stations 1, 2 and 3 in the southern part (Fig. Supplementary Fig. 2). The surface DO exhibited less latitudinal variation with a statistically insignificant (Mann–Whitney test, $P > 0.05$) difference between the north and the south regions (Fig. 3d). Along the vertical profile, the DO dropped sharply below 50 m and a hypoxic environment (<1 ml l^{-1}) was noticed below 125 m depth (Fig. 3d).

The mixed layer depth (MLD) varied between 11 m and 68 m (ave. 34 ± 19 m). Although the average MLD in the south (ave. 39 ± 24 m) was higher than the north (ave. 27 ± 8 m), the variation was statistically insignificant (Mann–Whitney test, $P > 0.05$). In the case of the bottom of the thermocline (BT), the depth varied between 119 and 149 m. Similar to MLD, the depth of the BT was higher (Mann–Whitney test, $P < 0.05$) in the south (ave. 142 ± 7 m) compared to the northern part (ave. 123 ± 6 m).

3.3. Phytoplankton biomass

In general, the surface chlorophyll *a* (phytoplankton biomass) was observed to be low (<0.5 mg m^{-3}) in the study region (Fig. 5). Along the meridional scale, the surface chlorophyll *a* was relatively high in the southern regions (ave. 0.21 ± 0.02 mg m^{-3})

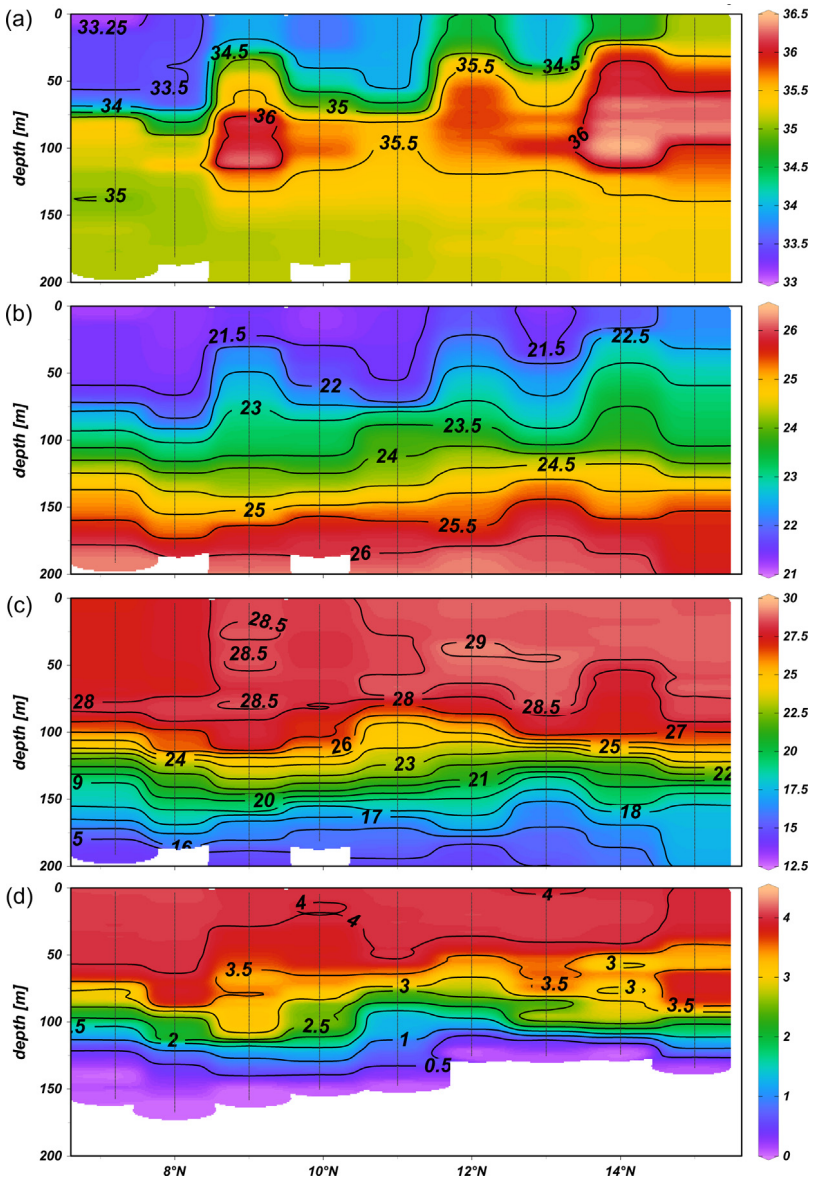

Fig. 3. Vertical distribution of (a) salinity, (b) potential density [g cm^{-3}], (c) temperature [°C] and (d) Dissolved Oxygen [ml l^{-1}] along the eastern Arabian Sea.

than the north (ave. 0.17 ± 0.01 mg m^{-3}) and the variation was found to be statistically significant (Mann–Whitney test, $P < 0.05$) (Fig. 5).

3.4. Zooplankton biomass and abundance

Zooplankton biomass and abundance exhibited conspicuous variation both along the latitudes and depth layers (Fig. 6). Among the three sampling depths, zooplankton biomass and abundance was relatively high in the MLD (ave. 0.15 ± 0.09 ml m^{-3}, and 520 ± 345 ind m^{-3}, respectively) than the TC (ave. 0.08 ± 0.05 ml m^{-3}, and 215 ± 130 ind m^{-3}, respectively) and the BTB (ave. 0.13 ± 0.19 ml m^{-3}, and 71 ± 65 ind m^{-3}, respectively) and the variations were statistically significant (Friedman test, $P < 0.05$). In MLD, excluding station 2, the zooplankton biomass and abundance was markedly high in the south (ave. 0.21 ± 0.11 ml m^{-3}, and 809 ± 288 ind m^{-3}, respectively) compared to the north (ave. 0.11 ± 0.02 ml m^{-3}, and 309 ± 175 ind m^{-3}, respectively) with a statistically significant variation (Mann–Whitney test, $P < 0.05$). In the deeper strata, though the biomass and abundances were relatively higher in the southern part, the variations were statistically insignificant (Mann–Whitney test, $P > 0.05$) (Fig. 6).

3.5. Zooplankton composition

A total of 27 zooplankton taxa were observed during the study (Table 1). The number of taxa observed was relatively high in the upper two depth layers (23 both in MLD and TC) compared to the bottom layer (15 in BTB). Cladocera and Lamellibranch larvae were observed only in MLD whereas Luciferiidae and Ctenophora were observed only in the TC stratum. Although, Copepoda dominated in all the depth layers, their abundance (496.4 ± 330.4, 201 ± 125.8, 61.4 ± 61 ind m^{-3}, in MLD, TC, and BTB, respectively) and contribution to the total zooplankton population along each stratum (95.5, 93.5, and 86.5%, in MLD, TC, and BTB, respectively) decreased gradually with depths. Chaetognatha, Siphonophorae, Hydrozoa, Decapoda larvae, and Polychaete larvae were the other abundant taxa present in all the three depth strata (Table 1). In MLD, the depth at which the intrusion of the BoB water was most evident, the number of taxa observed was 18 and 20 in the southern and northern part, respectively (Table 1). Salpa, Pteropoda and Amphioxus, were observed only in the MLD of south whereas Cladocera, Gastropoda larvae, Lamellibranch larvae, and Stomatopoda were

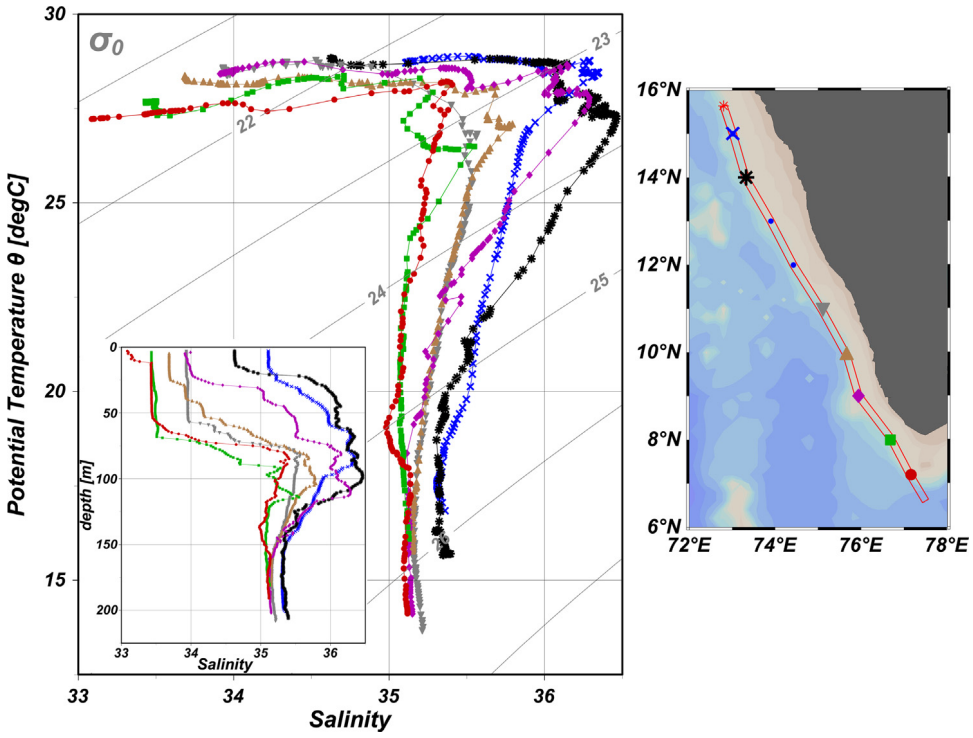

Fig. 4. T-S diagrams exhibiting water properties along the station locations. Inset: Vertical profile of salinity along the station locations in the eastern Arabian Sea.

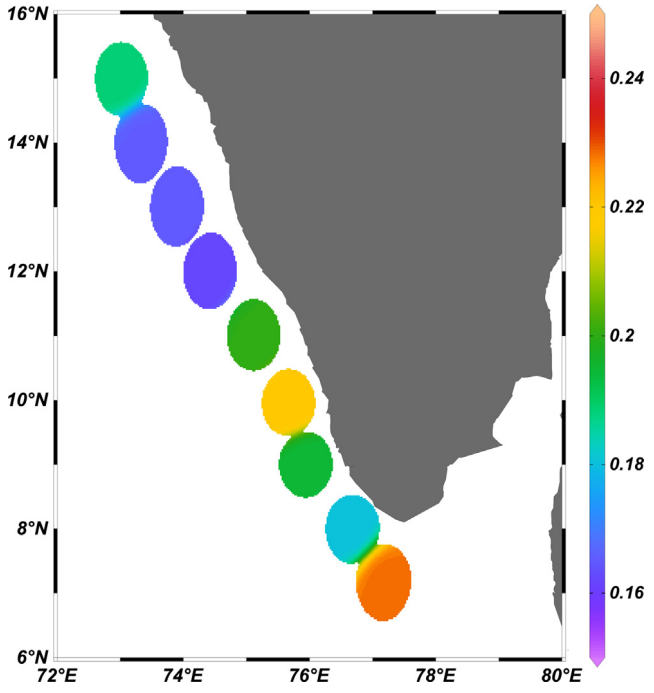

Fig. 5. Distribution of Chlorophyll *a* (mg m^{-3}) along the eastern Arabian Sea.

Table 1
The abundance of zooplankton taxa in the mixed layer depth (MLD), thermocline (TC) and the base of the thermocline to near bottom (BTB) of the eastern Arabian Sea (abundance ± std. deviation, unit - ind m^{-3}).

Taxa	MLD	TC	BTB
Copepoda	496 ± 330	201 ± 126	61 ± 61
Chaetognatha	9.6 ± 10	6.6 ± 5.2	2.6 ± 1.8
Copelata	3.5 ± 8	1.2 ± 1.7	0
Ostracoda	0.3 ± 0.4	0.5 ± 0.4	1.9 ± 2.1
Amphipoda	0.37 ± 0.38	0.39 ± 0.59	0.06 ± 0.12
Euphausiida	0.15 ± 0.37	0.19 ± 0.3	1 ± 2
Decapoda larvae	3 ± 4	1.7 ± 1.9	2.4 ± 3.8
Mysida	0.1 ± 0.2	0.8 ± 1	0.04 ± 0.09
Lucifer	0	0.02 ± 0.03	0
Cladocera	0.025 ± 0.07	0	0
Salpa	0.21 ± 0.48	0.004 ± 0.01	0
Polychaeta	0.72 ± 1.25	0.53 ± 0.44	0.3 ± 0.5
Doliolida	0.29 ± 0.44	0.15 ± 0.23	0
Fish eggs	0.79 ± 1.2	0.04 ± 0.08	0
Fish Larvae	0.23 ± 0.37	0.24 ± 0.27	0.03 ± 0.06
Ctenophora	0	0.03 ± 0.06	0
Siphonophora	1.97 ± 2.7	0.71 ± 0.61	0.48 ± 0.7
Hydrozoa	0.57 ± 0.9	0.63 ± 0.55	0.31 ± 0.53
Foraminifera	0	0	0
Gastropoda larvae	0.185 ± 0.56	0.012 ± 0.03	0.351 ± 1
Bivalve larvae	0.247 ± 0.74	0	0
Pteropoda	0.223 ± 0.47	0.08 ± 0.16	0.006 ± 0.02
Cephalopoda	0.05 ± 0.09	0.03 ± 0.06	0
Echinoderm larvae	0	0.096 ± 0.15	0.12 ± 0.18
Amphioxus	0.046 ± 0.14	0.052 ± 0.1	0.007 ± 0.02
Stomatopoda	0.012 ± 0.037	0.013 ± 0.039	0
Unidentified nauplii	0.59 ± 1.7	0	0

observed only in the northern part. Although, Copepoda formed the dominant zooplankton taxon in both regions, their abundance was higher in the south (657.7 ± 352 ind m^{-3}) compared to the north (295 ± 168 ind m^{-3}). Except for Ostracoda, Mysidacea, Doliolida and Decapoda larvae, all the other taxa which were present in both north and south (total 11) exhibited high abundance in the south compared to its counterpart (Table 1).

3.6. Copepoda community structure

A total of 57 copepod species were observed in the region of which only 33 species were common to all three depth strata (Table 2). The number of species observed was relatively higher in MLD (49) and BTB (48) than the TC stratum (44). *Paracalanus parvus* formed the dominant species in all the three depth strata followed by *Oncaea venusta* (Table 2). A total of seven species

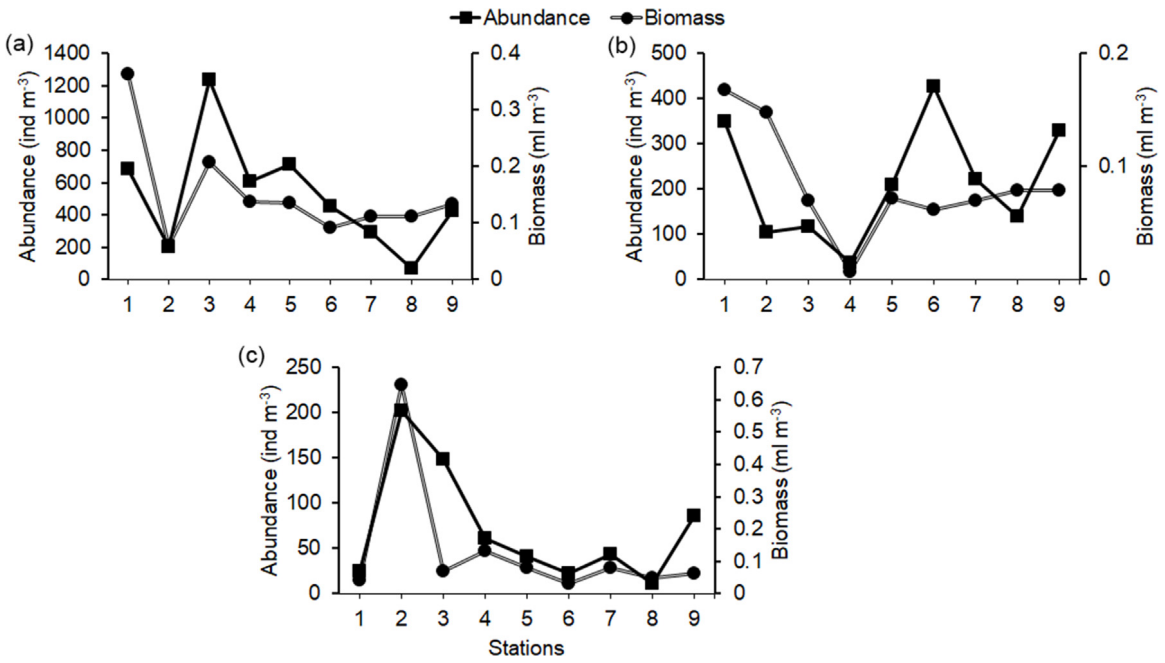

Fig. 6. Distribution of mesozooplankton biomass (ml m^{-3}) and abundance (ind m^{-3}) at (a) MLD, (b) TC and (c) BTB.

were observed only in the MLD whereas in case of TC and BTB strata the number of species exclusively observed was 4 and 3, respectively (Table 2). In MLD, where the BoB water intrusion was prominent, the number of species was relatively high in the south (41) compared to the north (37) (Supplementary Table 1). *P. parvus* dominated in both regions (58.8% and 65.6%, in south and north, respectively) and the other abundant species (>1%) common to both regions were *O. venusta, Paracalanus aculeatus*, and *Oncaea media*. The species which were abundant (>1%) only in the south were *Acrocalanus longicornis* and *Cosmocalanus darwinii* whereas in the north species like *Euchaeta rimana, Oithona similis, Farannula gibbula,* and *Corycaeus catus* (Supplementary Table 1) dominated. Among the abundant species, A. longicornis was observed exclusively in the first two sampling stations (St 1 and St 2) of the south. In MLD, a total of 12 species were observed only in the south and in the north the number was 8 (Supplementary Table 1).

3.7. Data analyses

In one-way ANOSIM analysis, the copepod community along three depth layers were found to be significantly distinguishable from each other (Global R = 0.261, p = 0.001). The pairwise tests among the depth layers also exhibited significant difference in the community structure between each pair of the depth strata (MLD and TC: R statistic = 0.235, p = 0.003; MLD and BTB: R statistic = 0.417, p = 0.001; TC and BTB: R statistic = 0.169, p = 0.013). Considering the spatial variation in the community structure of copepod within the MLD, it was observed that the copepod community in the south were significantly distinguishable from that of the north (Global R = 0.519, p = 0.008).

Based on 65% similarity, three clusters were observed based on the abundance of Copepoda species in the MLD (Fig. 7). The large cluster (cluster I) was formed by 5 locations in the south. Of the two small clusters, one was formed by stations 6 and 7 in the north (cluster II) and another one by the northern-most two locations (cluster III, Fig. 7).

The k-dominance plot exhibited a detailed picture of the copepod species diversity within MLD (Fig. 8). The copepod diversity was high in most of the stations in the south (except St 2) (Fig. 8).

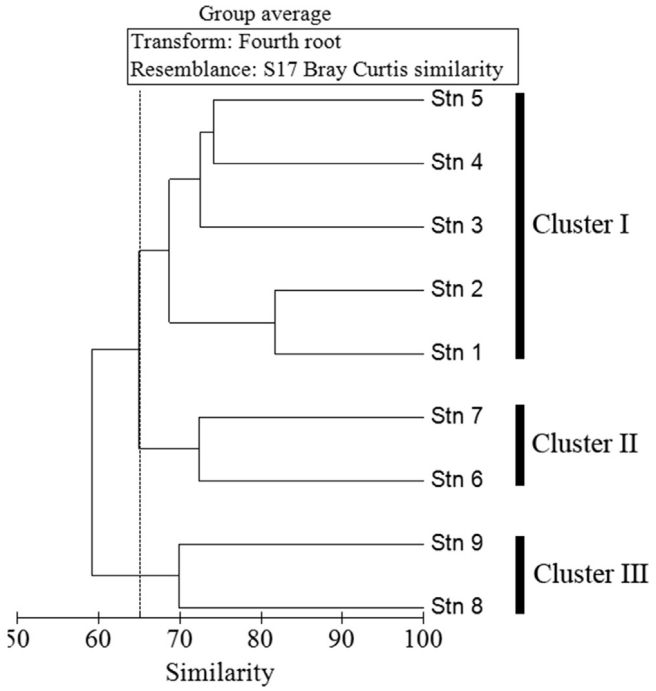

Fig. 7. Dendrogram of the station locations based on the abundance of the species of Copepoda in the MLD.

The variability observed in the copepod community structure in the MLD was further evaluated using the MVDISP algorithm. The variability was high in the sampling locations in the south (Dispersion factor value = 1.353), compared to the locations in the north (Dispersion factor value = 0.788). The Index of Multivariate Dispersion (IMD) exhibited a negative value (−0.6) in the pairwise comparisons among the south, and the north locations.

The result of the Bio-Env analysis indicated that the combination of salinity and chlorophyll *a* formed the most important factor (corr. 0.333) that best explained the variability in

Table 2
The abundance of Copepoda species in the mixed layer depth (MLD), thermocline (TC) and the base of the thermocline to near bottom (BTB) of the eastern Arabian Sea.

Copepods	MLD	TC	BTB
Undinula vulgaris	5.839	2.438	1.028
Canthocalanus pauper	1.363	0.565	0.321
Nannocalanus minor	2.262	0.836	0.535
Scolecithrix danae	0.761	0.459	0.146
Subeucalanus subtenuis	0.513	0.118	0
Subeucalanus crassus	0.467	0	0.483
Subeucalanus subcrassus	0.509	0.169	0.003
Subeucalanus mucronatus	0	1.393	0
Subeucalanus pileatus	0.332	0.181	0.052
Eucalanus elongatus	0.107	0.057	0.112
Eucalanus attneuates	1.548	0.085	0.102
Rhincalanus nasutus	0	0	0.003
Paracalanus parvus	300.9	129.3	32.36
Paracalanus aculeatus	10.27	5.095	1.577
Paracalanus indicus	0	0	0.186
Acartia gracilis	1.753	0.543	0.301
Acrocalanus monachus	0.228	0.052	0.014
A. longicornis	6.922	0.386	0
Cosmocalanus darwinii	4.707	0.577	0.617
Metacalanus aurivilli	0	0.009	0.016
Euchirella pulchra	0	0.003	0
Gaetanus minor	0.033	0	0.009
Euchaeta concinna	0.281	0.706	0.194
Euchaeta rimana	3.494	1.858	4.816
Temora turbinata	0.1	0	0
Temora discaudata	0.459	0.037	0.057
Pleuromamma indica	0	0	0.147
Pleuromamma abdominalis	0.382	0	0.653
Pleuromamma xiphias	0	0.009	0
Pleuromamma spinifera	0	0.009	0
Candacia catula	0.886	0.212	0.131
Candacia curta	1.67	0.196	0.038
Labidocera minuta	0.038	0	0
Labidocera spp	0.041	0	0
Calanopia elliptica	0.121	0.105	0
Calanopia minor	0.117	0.029	0.043
Pontellina plumata	0.604	0.175	0.042
Pontellopsis macronyx	0.031	0	0
Centropages furcatus	0.038	0.016	0
Centropages calaninus	0.06	0	0
Centropages gracilis	0.066	0.028	0
Pseudodiaptomus serricaudatus	0.15	0	0
Acartia danae	1.381	0.218	0.201
Acartia erythraea	0.03	0	0
Lucicutia flavicornis	0.548	0.19	0.662
Macrosetella gracilis	1.32	0.149	0.107
Microsetella norvegica	0.209	0.024	0.024
Oncaea venusta	117.1	42.08	11.43
Oncaea media	12.89	8.15	1.819
Oithona plumifera	1.061	0.405	0.071
O. similis	5.045	1.471	0.843
Farranula gibbula	2.707	0.412	0.279
Corycaeus catus	4.716	1.253	1.297
Corycaeus speciosus	0.684	0.354	0.058
Copilia mirabilis	0.085	0.18	0
Sapphirina spp	0.82	0.075	0.107
Clytemnestra scutellata	0.864	0.336	0.542

the abundance and community structure of the copepods in the MLD (Supplementary Table 2). The RDA triplot exhibited the preferred environment for the copepod species (Fig. 9). Three unique groups were identified based on their preference towards the abiotic environments. The first group containing nine copepod species had a preference for low salinity and density (Fig. 9). The second group with five species was positively correlated with salinity. The four species in the third group were positively correlated with density and negatively related to temperature and DO (Fig. 9).

4. Discussion

The dynamic coastal currents exhibiting conspicuous spatiotemporal variation in their strength and direction often form a prime determinant shaping the coastal hydrography and its biotic inhabitants (Daneri et al., 2000; Hwang and Wong, 2005). EICC and WICC, the two important coastal currents flowing along the east and west coast of India had a determining role in the water mass characteristics along the west coast of India. The low saline (<34) and less dense (<22.5 g cm^{-3}) water present in the upper 50 m water column in the south (up to 11° N) represented the intrusion of the BoB water into the AS. The southward direction of EICC, the joining of EICC to the coastal currents in the west and the northward direction of the WICC (Fig. 2) evince the intrusion of BoB water mass into the AS. Considering the temporal variation in the currents in response to the seasonal fluctuations, the current pattern for one more year was also analyzed to get a clear picture (Supplementary Fig. 3). The characteristics of current in 2018 were similar and followed the general pattern of the northeast monsoon period. The slight local invariability in the magnitude and the direction of these currents might have happened by the variation in the regulating factors like the local and remote forcing interior Ekman pumping and coastally-trapped Kelvin waves (McCreary et al., 1996; Shetye, 1998).

The vertical structure of the AS water column is considered to be influenced by several distinct water masses, each of them characterized by specific salinity, temperature and density profiles (Prasad et al., 2001). In our study also, the subsurface water (50–125 m) characterized by high salinity (>35.6) and potential density of 22.8–24.5 g cm^{-3}, and temperature of 24°–28 °C satisfied the characteristics of Arabian Sea High Saline Water (Prasanna Kumar and Prasad, 1999) and was reasonably distinct from the surface waters. This high saline dense water is formed in the northern Arabian Sea due to the enhanced evaporation by the dry continental wind from the northeast during winter monsoon and subsequently, sinks as the density increases with increase in salinity. This water mass influenced by the Findlater jet (Somali Jet) flows towards south during summer monsoon and triggers the WICC. The water mass sinks to deeper layers (50–150 m) as it progresses to the south (Shenoi et al., 1993; Prasanna Kumar and Prasad, 1999). The weak subsurface temperature inversion observed in most of the locations (Supplementary Fig. 2) might have happened by the sinking of this water mass in the north and the resultant southward flow of the surface waters as the subsurface water mass. The distinct nature of the deeper water (125–200 m) characterized by medium salinity (34.5–35.5) proves the existence of three distinct water masses within the depth of 200 m and corroborated the view of the co-existence of different water masses along the vertical axis of the AS (Rochford, 1964). However, deep water masses like Red Sea water (temperature 13°–19 °C, salinity 35.1–37.9 and potential density 26.2–26.8 g cm^{-3}) and Persian Gulf water (temperature 9°–11 °C, salinity 35.1–35.6 and potential density 27–27.4 gm cm^{-3}, (Prasanna Kumar and Prasad, 1999) were not observed in this region during the study period. Considering the depths of the study locations (∼200 m), their occurrence during the present study can be ruled out as these two water masses are mostly confined at deeper depths of 200–400 m (Persian Gulf water) and 500–800 m (Red Sea water) in the eastern Arabian Sea (Prasad et al., 2001).

Because of the northward intrusion of the BoB water into the AS, a gradual increase in the salinity is expected in the surface waters from south to north. Although this trend was present in the salinity distribution, along 9° and 12° N, the surface water salinity was slightly higher than the expected (Fig. 3). The offshore-deflection of the northward movement of the WICC along 9° and

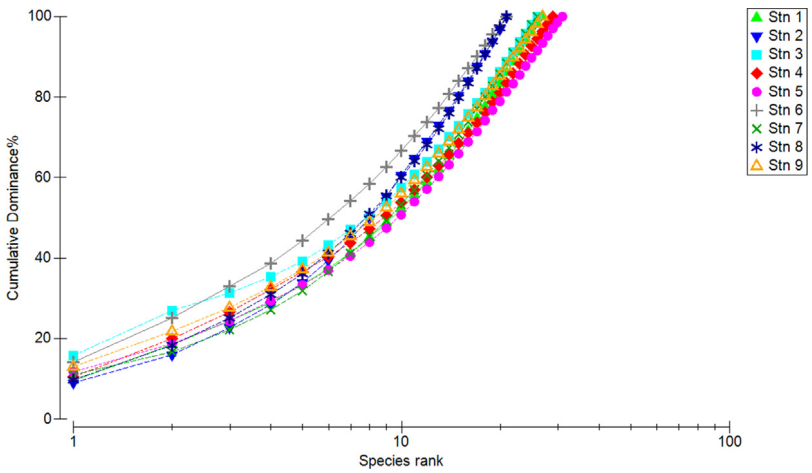

Fig. 8. k-dominance plot based on the abundance of the species of Copepoda in the mixed layer depth of the station locations in the eastern Arabian Sea.

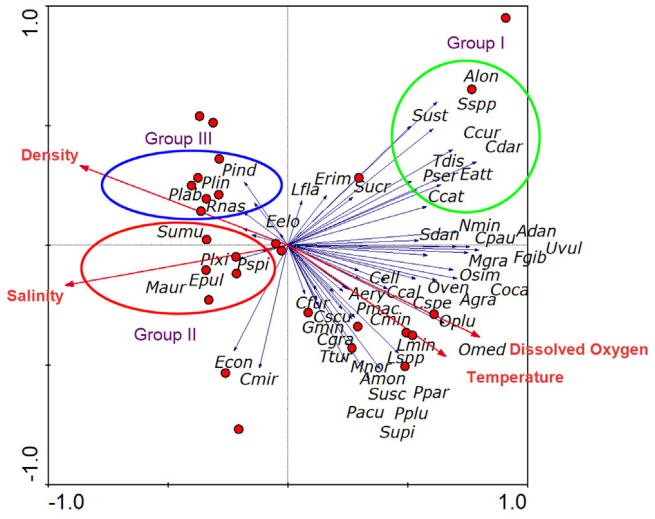

Adan - *Acartia danae*	Eatt - *Eucalanus attneuates*	Ppar - *Paracalanus parvus*
Aery - *Acartia erythraea*	Eelo - *Eucalanus elongatus*	Plab - *Pleuromamma abdominalis*
Agra - *Acartia gracilis*	Epul - *Euchirella pulchra*	Plin - *Pleuromamma indica*
Alon - *Acrocalanus longicornis*	Erim - *Euchaeta rimana*	Plxi - *Pleuromamma xiphias*
Amon - *Acrocalanus monachus*	Fgib - *Farranula gibbula*	Pmac - *Pontellopsis macronyx*
Ccal - *Centropages calaninus*	Gmin - *Gaetanus minor*	Pplu - *Pontellina plumata*
Ccat - *Candacia catula*	Lfla - *Lucicutia flavicornis*	Pser - *Pseudodiaptomus serricaudatus*
Ccur - *Candacia curta*	Lmin - *Labidocera minuta*	Pspi - *Phaenna spinifera*
Cdar - *Cosmocalanus darwinii*	Lspp - *Labidocera* spp	Rnas - *Rhincalanus nasutus*
Cell - *Calanopia elliptica*	Maur - *Metacalanus aurivilli*	Sspp - *Sapphirina* spp
Cfur - *Centropages furcatus*	Mgra - *Macrosetella gracilis*	Sdan - *Scolecithrix danae*
Cgra - *Centropages gracilis*	Mnor - *Microsetella norvegica*	Sucr - *Subeucalanus crassus*
Cmin - *Calanopia minor*	Nmin - *Nannocalanus minor*	Sumu - *Subeucalanus mucronatus*
Cmir - *Copilia mirabilis*	Omed - *Oncaea media*	Supi - *Subeucalanus pileatus*
Coca - *Corycaeus catus*	Oplu - *Oithona plumifera*	Sust - *Subeucalanus subtenuis*
Cpau - *Canthocalanus pauper*	Osim - *Oithona similis*	Susc - *Subeucalanus subcrassus*
Cscu - *Clytemnestra scutellata*	Oven - *Oncaea venusta*	Tdis - *Temora discaudata*
Cspe - *Corycaeus speciosus*	Pacu - *Paracalanus aculeatus*	Ttur - *Temora turbinata*
Econ - *Euchaeta concinna*	Pind - *Paracalanus indicus*	Uvul - *Undinula vulgaris*

Fig. 9. The RDA triplot displaying the association of the Copepoda species with the abiotic variables.

12° N might have contributed to this apparent variation in the salinity distribution. This observation further substantiates the influence of coastal currents in the intrusion and distribution of BoB water into the AS.

The relatively high phytoplankton biomass observed in the surface waters of the southern AS compared to the north might be due to the increased nutrient availability in the buoyancy induced vertically mixed water originated in the south of Indo-Srilanka channel. During winter, before the BoB water enters the AS, a mini cold pool builds up in the southwest part of Srilanka contributing to buoyancy-driven vertical mixing (Rao et al., 2008). The EICC helps in bringing this water to south-eastern AS. Although, the nutrient analysis was not carried out in the present study, considering the physical process active in this region, the observation of the north–south variation in the phytoplankton biomass concurrent to the nutrient advection seems to be reasonable.

Zooplankton biomass and abundance were also significantly high in the south compared to the north in the MLD signifying the role of the enhanced phytoplankton biomass in sustaining the higher zooplankton abundance in the south. The role of coastal currents contributing to the heterogeneity in the abundance of zooplankton community has been recorded from many coastal and shelf regions around the world (Valentin and Monteiro-Ribas, 1993). Considering the depth of the mixed layer (range 11–68 m), and the thickness of the intruded water (∼50 m), the zooplankton distribution in the MLD was suitable to explain the influence of the intrusion of the BoB water into the coastal AS. The observed higher abundance of the majority of the zooplankton taxa clearly indicated the positive influence of the intrusion in the MLD of the southern part of the AS. Of the 23 zooplankton taxa observed in the MLD, only 15 taxa were common to both the northern and southern part. The discrete nature of the two water masses along the northern and southern parts of the AS might have contributed for this difference in the zooplankton community composition.

The conspicuous difference observed in the zooplankton biomass and abundance along the three depth layers (MLD, TC, and BTB) substantiates the role of discrete water masses in structuring the zooplankton community of the AS. Considering the depth of the top (12–69 m) and bottom (119–149 m) of the TC, and taking into account the depth of the Arabian sea high saline water (50–125 m), the TC was considered as the most suitable to explain the zooplankton community composition of this high saline water mass. Similarly, the BTB was taken as a good representative of the intermediate saline bottom water. The variability in the abundance and community composition of the zooplankton taxa along these depth layers (Table 1) might be due to the differences in the association of zooplankton community to the discrete water masses in this coastal ecosystem.

Although the copepod abundance was markedly higher in the south compared to the north in the MLD, it was important to identify whether the enhanced abundance was contributed by the local population growth or by the advection with water masses associated with the BOB intrusion. Though the copepod, *P. parvus* formed the dominant species in both the regions, their twofold higher abundance in the south points towards a favorable environment for their population growth. Similarly, most of the species which were common to both regions in MLD had high abundance in the south. The relatively high phytoplankton biomass might have supported the higher abundance of these copepod species in the south. Moreover, the result of the BIOENV analysis in which, the combination of salinity and chlorophyll *a* was identified as the most important factor determining the copepod community strengthens the view. The crucial role of chlorophyll *a* in sustaining the higher abundance of copepods recorded from both the Indian waters and around the globe further substantiates the observation (Karati et al., 2018, 2019; Devreker et al., 2005). The salinity variability in the AS contributed by the intrusion of BoB water exerted a prominent influence on the copepod community.

Interestingly, the higher number of Copepoda species observed in the south (41) compared to the north (37) in the MLD might have resulted by the advection of organisms with the current flow. The k-dominance plot depicting relatively high number of species in many locations in the south (Fig. 8) also indicates the increase in species number with the mixing of the intruded water. The abundant species, *Acrocalanus longicornis* was observed only in the southern-most two stations (St 1 and St 2), where the intrusion depth was the maximum. This species has been recorded as the abundant species in the coastal waters of south-west BoB during winter (Fernandes and Ramaiah, 2014) and hence their presence only in the southern stations supports the role of the coastal currents in distributing this species to the coastal AS. Copepods having limited capability to withstand the current flow, can get transported to longer distances thereby extending their geographic distribution by the coastal currents (Hwang and Wong, 2005). Also, the discrete existence of 12 copepod species only in the southern AS of MLD further corroborates the influence of the coastal current and the associated intrusion in increasing the abundance and species diversity of the copepod community in the south. The high variability in the sampling locations in the south (Dispersion factor value = 1.353), compared to the north (Dispersion factor value = 0.788) estimated through the MVDISP analysis might be the result of this diverse community present in the south.

The distinct clusters of the station locations of the south and north based on the Copepoda species abundance in the MLD were the output of the discrete community structure of these two regions. The negative IMD value (−0.6) in the MVDISP analysis implied that the similarities in the copepod community in locations of both the northern and southern regions were greater than the similarities of the community structure between the two regions. This was expected as in the Indian waters, the copepod community between the shelf and coastal regions have been observed to exhibit >90% dissimilarity (Rakhesh et al., 2006).

In the present study, the three distinct groups of the copepod community formed in the RDA analysis provided noteworthy information regarding the biotic–abiotic interrelation of this region. The nine copepod species of the first group is reported to have a preference for low-saline and low-density environment and were mostly observed in the southern part of the MLD. Hence they can be taken as a good representatives of the BoB intruded water mass in the coastal AS. The second group formed by species like, *Pleuromamma xiphias* which has been recorded in the southwest Tyrrhenian Sea with salinity between 37.22–38.17 (Ehrhardt, 1967) and *Phaenna spinifera* observed in Red Sea waters with salinity 40.1–41 have a preference towards the high saline environment (Pradopor, 1983). The other remaining species in this group have been recorded mostly in the offshore waters of the Arabian Sea and hence the association of all these species with the Arabian Sea High Saline water mass can be linked to their species specific salinity preferences. The four copepod species in the third group was associated with the high density, intermediate saline, and low oxygenated environment. All these species were observed only in BTB, and among them, species such as *Pleuromamma indica* and *Pl. abdominalis* are earlier reported from the mesopelagic oxygen-deficient waters in the AS (Madhupratap and Haridas, 1990; Padmavati et al., 1998). Thus, they can be considered as good representatives of the oxygen deficient intermediate saline water mass observed below the thermocline in the AS.

In the coastal Arabian Sea, though the station depths were only ∼200 m, the presence of different water masses brought about wide variability in the vertical structure of the copepod community. The result of the ANOSIM analysis exhibiting good discrimination in the copepod community structure among the depth layers (Global R = 0.261, p = 0.001) signifies the association of discrete species with the different water masses in this region. Earlier, the study on this dominant zooplankton taxon in the upper 1000 m of the AS revealed the depthwise distribution of copepods (Padmavati et al., 1998). The present study helped further to enhance the knowledge on the influence of different water masses with distinct abiotic attributes within the 200 m depth structuring the copepod community in this dynamic coastal region of the northern Indian Ocean.

5. Conclusion

Studies detailing the mechanisms that drive the asymmetry in the distribution of the water mass leading to conspicuous heterogeneity in the biotic community are essential in unraveling the ecological functioning of marine ecosystems. The upper layer of the southern part of the coastal AS experienced the intrusion of the low saline BoB water as a consequence of the southward flow of EICC, its feed to WICC and the northward flow of the WICC during the winter monsoon. This resulted in a conspicuous spatial invariability in the physicochemical environments of the upper layers of this region. The presence of the Arabian Sea High saline water mass in the mid-depths and the occurrence of the intermediate saline water in the bottom led to distinctness in the water mass characteristics. The cumulative effect of the horizontal advection by the coastal currents and the local population growth of the zooplankton community supported by the moderately higher phytoplankton preponderances resulted in higher zooplankton biomass and abundance in the south compared to the northern AS. The heterogeneity in the hydrographical characteristics of discrete water masses governed the community composition and distribution of the dominant zooplankton taxon, Copepoda in this coastal ecosystem. The present study detailing the influence of the coastal circulation in defining the water mass characteristics and identifying the associated zooplankton community dynamics will improve the understanding of the macroecology of this dynamic and economically valuable marine habitat in the northern Indian Ocean.

Declaration of competing interest

The authors declare that they have no conflict of interest.

CRediT authorship contribution statement

Kusum Komal Karati: Formal analysis, Writing. **Ashadevi C.R.:** Conceptualization, Writing. **Rasheed K.:** Formal analysis, Supervision, Writing. **Vineetha G.:** Formal analysis, Writing. **Smitha B.R.:** Formal analysis, Writing. **Vimalkumar K.G.:** Supervision. **Sari Mol C.N.:** Formal analysis. **Sudhakar M.:** Conceptualization, Writing.

Acknowledgments

This study was carried out as part of the Monitoring and Modeling of Marine Ecosystem, Marine Living Resources Program (MMME – MLR), of the Ministry of Earth Sciences, Government of India, New Delhi implemented by the Centre for Marine Living Resources and Ecology (CMLRE), Kochi. The authors acknowledge all participants of Cruise 355 of FORV *Sagar Sampada* for their support and help rendered during sampling onboard. This is CMLRE contribution no 104.

Appendix A. Supplementary data

Supplementary material related to this article can be found online at https://doi.org/10.1016/j.rsma.2019.100761.

References

Anderson, M.J., Crist, T.O., Chase, J.M., Vellend, M., Inouye, B.D., Freestone, A.L., Sanders, N.J., Cornell, H.V., Comita, L.S., Davies, K.F., Harrison, S.P., 2011. Navigating the multiple meanings of β diversity: A roadmap for the practicing ecologist. Ecol. Lett. 14, 19–28.

Ayón, P., Criales-Hernandez, M.I., Schwamborn, R., Hirche, H.J., 2008. Zooplankton research off peru: A review. Prog. Oceanogr. 79 (2–4), 238–255.

Barnes, R.S.K., Hughes, R.N., 1999. An Introduction to Marine Ecology, third ed. Blackwell Publishing, Oxford, UK.

Bonnet, D., Frid, C., 2004. Seven copepod species considered as indicators of water-mass influence and changes: Results from a Northumberland coastal station. ICES J. Mar. Sci. 61 (4), 485–491.

Caputi, N., Fletcher, W.J., Pearce, A., Chubb, C.F., 1996. Effect of the Leeuwin Current on the recruitment of fish and invertebrates along the Western Australian coast. Mar. Freshw. Res. 47 (2), 147–155.

Clarke, K.R., Gorley, R.N., 2015, PRIMER v7: User Manual/Tutorial. PRIMER-E, Plymouth.

Clarke, K.R., Somerfield, P.J., Gorley, R.N., 2008. Testing of null hypotheses in exploratory community analyses: Similarity profiles and biota-environment linkage. J. Exp. Mar. Biol. Ecol. 366 (1–2), 56–69.

Conway, D.V.P., White, R.G., Hugues-Dit-Ciles, J., Gallienne, C.P., Robins, D.B., 2003. Guide to the Coastal and Surface Zooplankton of the South-Western Indian Ocean. Marine Biological Association of the United Kingdom, Plymouth.

Daneri, G., Dellarossa, V., Quiñones, R., Jacob, B., Montero, P., Ulloa, O., 2000. Primary production and community respiration in the Humboldt Current System off Chile and associated oceanic areas. Mar. Ecol. Prog. Ser. 197, 41–49.

Devreker, D., Souissi, S., Seuront, L., 2005. Effects of chlorophyll concentration and temperature variation on the reproduction and survival of Temora longicornis (Copepoda, Calanoida) in the Eastern English Channel. J. Exp. Mar. Biol. Ecol. 318, 145–162.

Ehrhardt, J.P., 1967. Contribution à l'étude du plancton superficiel et subsuperficiel du canal de Sardaigne et de la mer sudtyrrhénienne. Cah. Océanogr. 19, 657–921.

Eisner, L., Hillgruber, N., Martinson, E., Maselko, J., 2013. Pelagic fish and zooplankton species assemblages in relation to water mass characteristics in the northern Bering and southeast Chukchi seas. Polar Biol. 36 (1), 87–113.

Fernandes, V., Ramaiah, N., 2014. Distributional characteristics of surface-layer mesozooplankton in the Bay of Bengal during the 2005 winter monsoon. Indian J. Geo-Mar. Sci. 43, 176–188.

Gauns, M., Madhupratap, M., Ramaiah, N., Jyothibabu, R., Fernandes, V., Paul, J.T., Kumar, S.P., 2005. Comparative accounts of biological productivity characteristics and estimates of carbon fluxes in the Arabian Sea and the Bay of Bengal. Deep Sea Res. II 52, 2003–2017.

Harris, R., Wiebe, P., Lenz, J., Skjoldal, H.R., Huntley, M. (Eds.), 2000. ICES Zooplankton Methodology Manual. Academic Press, London, p. 684p.

Hwang, J.S., Wong, C.K., 2005. The China Coastal Current as a driving force for transporting Calanus sinicus (Copepoda: Calanoida) from its population centers to waters off Taiwan and Hong Kong during the winter northeast monsoon period. J. Plankton Res. 27 (2), 205–210.

Karati, K.K, Vineetha, G., Raveendran, T.V., Dineshkumar, P.K., Muraleedharan, K.R., Joseph, T., Jayalakshmi, K.V., 2019. Implications of a regional-scale process (the Lakshadweep low) on the mesozooplankton community structure of the Arabian sea. Mar. Freshw. Res. 70, 345–358.

Karati, K.K., Vineetha, G., Raveendran, T.V., Muraleedharan, K.R., Habeebrehman, H., Philson, K.P., Achuthankutty, C.T., 2018. River plume fronts and their implications for the biological production of the Bay of Bengal. Indian Ocean. Mar. Ecol. Prog. Ser. 597, 79–98.

Kasturirangan, L.R., 1963. A Key for the Identification of the more Common Planktonic Copepod of Indian Coastal Waters. Council of Scientific and Industrial Research, New Delhi.

Luis, A.J., Kawamura, H., 2004. Air-sea interaction, coastal circulation and primary production in the eastern Arabian Sea: A review. J. Oceanogr. 60 (2), 205–218.

Madhupratap, M., Gopalakrishnan, T.C., Haridas, P., Nair, K.K.C., Aravindakshan, P.N., Padmavati, G., Paul, S., 1996. Lack of seasonal and geographic variation in mesozooplankton biomass in the Arabian Sea and its structure in the mixed layer. Curr. Sci. 71, 863–868.

Madhupratap, M., Haridas, P., 1990. Zooplankton, especially calanoid copepods, in the upper 1000 m of the south-east Arabian Sea. J. Plankton Res. 12, 305–321.

McCreary, J.P., Han, W., Shankar, D., Shetye, S.R., 1996. Dynamics of the east India coastal current: 2. numerical solutions. J Geophys. Res.: Oceans 101 (C6), 13993–14010.

Padmakumar, K.B., Thomas, L.C., Vimalkumar, K.G., Devi, C.A., Maneesh, T.P., Vijayan, A., Gupta, G.V.M., Sudhakar, M., 2017. Hydrobiological responses of the North Eastern Arabian Sea during late winter and early spring intermonsoons and the repercussions on open ocean blooms. J. Mar. Biol. Assoc. UK 97 (7), 1467–1478.

Padmavati, G., Haridas, P., Nair, K.K.C., Gopalakrishnan, T.C., Shiney, P., Madhupratap, M., 1998. Vertical distribution of mesozooplankton in the central and eastern Arabian Sea during the winter monsoon. J. Plankton Res. 20 (2), 343–354.

Paffenhöfer, G.A., Knowles, S.C., 1980. Omnivorousness in marine planktonic copepods. J. Plankton Res. 2, 355–365.

Pauly, D., Christensen, V., Guénette, S., Pitcher, T.J., Sumaila, U.R., Walters, C.J., Watson, R., Zeller, D., 2002. Towards sustainability in world fisheries. Nature 418 (6898), 689–695.

Pradopor, M., 1983. The diversity and dynamics of calanoida (copepoda) in the northern gulf of elat (aqaba), red-sea. Oceanol. Acta 6 (2), 139–145.
Prasad, T.G., Ikeda, M., Prasanna Kumar, S., 2001. Seasonal spreading of the Persian Gulf Water mass in the Arabian Sea. J. Geophys. Res. Oceans 106 (C8), 17059–17071.
Prasanna Kumar, S., Narvekar, J., Kumar, A., Shaji, C., Anand, P., Sabu, P., Rijomon, G., Josia, J., Jayaraj, K.A., Radhika, A., Nair, K.K.C., 2004. Intrusion of the Bay of Bengal water into the Arabian Sea during winter monsoon and associated chemical and biological response. Geophys. Res. Lett. 31 (15).
Prasanna Kumar, S., Prasad, T.G., 1999. Formation and spreading of Arabian Sea high-salinity water mass. J. Geophys. Res. Oceans 104 (C1), 1455–1464.
Rakhesh, M., Raman, A.V., Sudarsan, D., 2006. Discriminating zooplankton assemblages in neritic and oceanic waters: a case for the northeast coast of india, bay of bengal. Mar. Env. Res. 61, 93–109.
Rao, R.R., GirishKumar, M.S., Ravichandran, M., Gopalakrishna, V.V., Thadathil, P., 2008. A cold pool south of Indo-SriLanka channel and its intrusion into the southeastern Arabian Sea during winter. Deep-Sea Res. I 55, 1009–1020.
Rochford, D.J., 1964. Salinity maxima in the upper 1000 metres of the north Indian ocean. Mar. Freshw. Res. 15 (1), 1–24.
Sewell, R.B.S., 1999. The Copepod of Indian Seas. Biotech Books, Delhi.
Shenoi, S.S.C., Shetye, S.R., Gouveia, A.D., Michael, G.S., 1993. Salinity Extrema in the Arabian Sea. University of Hamburg, vol. 76, pp. 37–49, (special Issue booklet).
Shetye, S.R., 1998. West India coastal current and Lakshadweep high/low. Sadhana 23 (5–6), 637–651.
Shetye, S.R., Gouveia, A.D., Shenoi, S.S.C., Michael, G.S., Sundar, D., Almeida, A.M., Santanam, K., 1991. The coastal current off western India during the northeast monsoon. Deep Sea Res. I 38 (12), 1517–1529.
Shetye, S.R., Shenoi, S.S.C., 1988. Seasonal cycle of surface circulation in the coastal north Indian ocean. Proc. Indian Acad. Sci. Earth Planet. Sci. 97 (1), 53–62.
Suthers, I.M., Rissik, D. (Eds.), 2009. Plankton: A Guide to their Ecology and Monitoring for Water Quality. CSIRO publishing, Collingwood, p. 255.
Thomas, K., Nielsen, T.G., 1994. Regulation of zooplankton biomass and production in a temperate, coastal ecosystem. 1. Copepods. Limnol. Oceanogr. 39 (3), 493–507.
Valentin, J.L., Monteiro-Ribas, W.M., 1993. Zooplankton community structure on the east-southeast Brazilian continental shelf (18–23° S latitude). Cont. Shelf Res. 13 (4), 407–424.
Verheye, H.M., Richardson, A.J., Hutchings, L., Marska, G., Gianakouras, D., 1998. Long-term trends in the abundance and community structure of coastal zooplankton in the southern Benguela system, 1951–1996. S. Afr. J. Mar. Sci. 19, 317–332.
Vineetha, G., Karati, K.K., Raveendran, T.V., Idreesbabu, K.K., Riyas, C., Muhsin, M.I., Shihab, B.K., Simson, C., Anil, P., 2018. Responses of the zooplankton community to peak and waning periods of El Niño 2015–2016 in Kavaratti reef ecosystem, northern Indian Ocean. Environ. Monit. Assess. 190, 465. http://dx.doi.org/10.1007/s10661-018-6842-9.
Warwick, R.M., Clarke, K.R., 1993. Taxonomic distinctness and environmental assessment. J. Appl. Ecol. 35, 532e543.
Wiafe, G., Frid, C.L.J., 1996. Short-term temporal variation in coastal zooplankton communities: The relative importance of physical and biological mechanisms. J. Plankton Res. 18 (8), 1485–1501.